DISCRETE AND CONTINUOUS
DYNAMICAL SYSTEMS SERIES S
Volume **8**, Number **5**, October **2015**

doi:10.3934/dcdss.2015.8.857

pp. **857–869**

ANNIHILATION OF TWO INTERFACES IN A HYBRID SYSTEM

Shin-Ichiro Ei and Kei Nishi

Department of Mathematics, Hokkaido University
Kita 10, Nishi 8, Kita ward, Sapporo, 060-0810, Japan

Yasumasa Nishiura

WPI Advanced Institute for Materials Research, Tohoku University
2-1-1 Katahira, Aoba-ku, Sendai 980-8577, Japan

Takashi Teramoto

Asahikawa Medical University
2-1-1-1, Midorigaoka-higashi, Asahikawa 078-8510, Japan

Abstract. We consider the mixed ODE-PDE system called a hybrid system, in which the two interfaces interact with each other through a continuous medium and their equations of motion are derived in a weak interaction framework. We study the bifurcation property of the resulting hybrid system and construct an unstable standing pulse solution, which plays the role of a separator for dynamic transition from standing breather to annihilation behavior between two interfaces.

1. **Introduction.** A propagating front of Allen-Cahn equation and pulse of the FitzHugh-Nagumo equations are classical examples of strong collision where annihilation of two colliding objects is observed, which has been regarded as a characteristic feature of dissipative waves. One of the recent remarkable developments for reaction-diffusion systems is the existence of invariant manifold for the motion of the colliding pair of traveling wave solutions sufficiently apart [4, 16, 17], which enables us to derive the equations of motion restricted on the center manifold [6]. Therefore, the head-on collision of counter-propagating particle-like patterns is a well-defined problem for scattering phenomena, which not only behave like elastic objects upon collision, but also scatter in various ways [13, 14].

In our previous study [12], we classified the propagating manners of traveling pulses when they encountered a jump-type heterogeneity, using the following bistable reaction-diffusion (RD) system:

$$\begin{cases} \tau\epsilon u_t = & \epsilon^2 u_{xx} + \left(u+\dfrac{1}{2}\right)\left(\dfrac{1}{2}-u\right)\left(u-\dfrac{1}{2}v\right), \\ v_t & = Dv_{xx} + u - v + \vartheta(x), \end{cases} \tag{1}$$

where the components $u = u(t,x)$ and $v = v(t,x)$ depend on time $t > 0$ and space $x \in \mathbf{R}$. For the parameters, we assumed $\tau > 0$, $0 < \epsilon \ll D$ and $\vartheta > 0$. The space-dependent function $\vartheta(x)$ was given by $\vartheta(x) = \vartheta^L + \varsigma/(1+\exp(-\gamma\, x))$ where

2010 *Mathematics Subject Classification.* Primary: 37L10, 35K57; Secondary: 37G10.

Key words and phrases. Dynamical system, reaction-diffusion, interface equation, annihilation dynamics.

γ is a positive constant, which changes continuously from ϑ^L to $\vartheta^L + \varsigma$ around the jump point $x = 0$, and the system becomes homogeneous at $x = \pm\infty$.

Although it is trivial that penetration occurs when a jump height ς is small, i.e., pulses can go across the low barriers, a variety of outputs appear depending on the parameter values τ and ς that include decomposition (DEC), rebound (REB), annihilation (ANN) (Fig.5(a) in [12]). In the previous study, we theoretically studied the underlying mechanism behind the DEC and REB behaviors. In particular, we performed center manifold reduction to clarify the sliding motion of a standing breather (SB) in the presence of jump-type heterogeneity. In fact, the REB regime can be replaced by the SB regime in the absence of heterogeneity as shown in Fig.4(a) in [12], in which the ANN regime was noted as the background (BG) regime. However, the theoretical details of the ANN behavior were left for future work.

Figure 1 (a) shows the spatio-temporal plot near the transition point between SB and ANN behaviors. Note here that we consider the dynamics in the homogeneous system at $x \to \infty$, so that we put $\vartheta(x) = \delta^L + \varsigma$ and $\delta^L = 0$. As ς was slightly below the transition point, transition from SB to ANN occurred. We carefully traced the orbital behavior near the transition point. It turned out that the orbit stayed very close to a quasi-steady state, then it either oscillated or annihilated depending on parameter values. In fact, it was also numerically confirmed that there existed a codimension one stationary pulse as shown in Fig. 1 (c)(d). It should be noted that this unstable stationary pulse can be numerically obtained by the continuation of a stable stationary pulse as in Fig. 17 in [12]. These numerical results indicate that the orbits are sorted out according to which side of the stable manifold it belongs. The destinations of the unstable manifold are ANN and SB behaviors, which can be confirmed also by numerics. It should be noted that the viewpoint of unstable objects called scattors is useful in understanding the output of collision dynamics accompanied by large deformation [1][2][13][14].

Our main concern in this paper is to construct an unstable stationary pulse which plays the role of scattors, based on a mixed ODE-PDE system called a hybrid system (HS), which is a singular limit system of the original RD (1) as the details will be given in Sec.2. The equation for the activator in the PDEs is just replaced by the ODEs for the motions of two interfaces in the HS. One of the benefits of reducing the RD system to HS is that it facilitates analytical treatment of the pulse dynamics. Actually, it allows us not only to investigate analytically the global existence and stability of stationary and traveling pulse solutions [9][15], but also to perform center manifold reduction with all the calculation done explicitly [3][12]. What is important about the hybrid system is that the pulse behaviors that occur for the original RD system are all reproduced for the hybrid system.

However, in the hybrid model which we studied in [12], the pulse was supposed to have annihilated when the interfaces cross each other. Therefore, the transition behavior from oscillation to annihilation in the hybrid system was different from that obtained in the original RD as shown in Fig. 1(a)(b). In fact, according to the numerical bifurcation analysis of the original RD system [12], the system typically has two stationary pulse solutions for the parameter regime we concerned, while the hybrid system has only one. It is analytically shown that there are no stationary solutions for the hybrid system associated with the codimension one pulse as in Fig. 1 (c)(d).

As a useful theoretical tool for characterizing such annihilation dynamics, the comparison theorem was employed to a scalar reaction-diffusion equation of the Allen-Cahn type for which the super- and sub-solutions are explicitly constructed for the colliding fronts concerned, thus showing the existence of an entire solution in between the two solutions [8][11]. The approach could not readily be extended to our two-component system, but the authors showed the existence of an unstable pulse solution considering the interaction term in equation of motion for colliding fronts. Therefore, the orbit of the colliding fronts coming from $x = \pm\infty$ passed through the lower side of the unstable solution at all times, eventually settled down to uniform background state.

In this paper, we rederive a hybrid system associated with the original RD system (1) on the basis of the weak-interaction framework [4][6], in which both of the interfaces are assumed to be so far apart that they are regarded as weakly coupled particles through the exponentially varying tails. We show that taking into account the interaction between two interfaces and modifying the equations of interface motion in the hybrid system improve the analytical results of the annihilation dynamics, in particular, of the transition mechanism between ANN-SB behaviors. We formally obtain the coefficients of the interaction terms for the modified hybrid system, which determine the interaction manner between the interfaces, hence the bifurcation properties of the pulse solution.

This paper is organized as follows: In section 2, we derive a modified hybrid system based on the weak-interaction framework. In section 3, we analytically investigate the existence and stability of stationary pulse solution to the modified hybrid system. Finally, in section 4, we make some remarks and discussions on the results obtained in the article.

2. **Derivation of modified hybrid system.** In the previous section, we saw that the unstable pulse solution called scattor played a central role in the ANN-SB transition for the pulse dynamics of the RD system. In the paper [12], we also introduced the following mixed ODE-PDE system

$$\begin{cases} \dot{\phi}_2 = -\dfrac{v(\phi_2)}{\sqrt{2\tau}}, \quad \dot{\phi}_1 = \dfrac{v(\phi_1)}{\sqrt{2\tau}}, \\ v_t = Dv_{xx} + u(x;\phi_2,\phi_1) - v + \vartheta(x), \end{cases} \tag{2}$$

where $x = \phi_2(t), \phi_1(t)$ $(\phi_1 \le \phi_2)$ are the location of the interfaces and the profile of the u-component $u(x;\phi_2,\phi_1)$ is now given by a piecewise-constant function

$$u(x;\phi_2,\phi_1) := H(x-\phi_1) - H(x-\phi_2) - 1/2, \tag{3}$$

where $H(x)$ is the Heaviside function: $H(x) = 0$ $(x < 0)$, 1 $(0 \le x)$. This system, which we called a hybrid system (HS), was obtained as a singular limit $\epsilon \searrow 0$ of the RD system (1) by following the method originally found in [7]. Since we restrict ourselves to the homogeneous case, we set $\vartheta(x) \equiv \vartheta = const.$ hereafter.

Let us review how the hybrid system (2) was derived. For later convenience, we rewrite the first equation in (1) for u-component in a general expression,

$$\tau\epsilon u_t = \epsilon^2 u_{xx} + f(u,v), \tag{4}$$

where $f(u,v) = (u+1/2)(1/2-u)(u-v/2)$. We remark that $f(-u,-v) = -f(u,v)$, $f_u(-u,-v) = f_u(u,v) = 1/4 - 3u^2 + uv$ and $f(P_\pm, v) = 0$ $(P_\pm = \pm 1/2)$ hold. We find that the scalar equation (4) with $v = v_I = const.$ has a traveling front solution connecting $P_\pm$ of the form $u = S(x - \phi(t))$ where $S(x) = -1/2 \tanh\left(x/2\sqrt{2}\epsilon\right)$ and

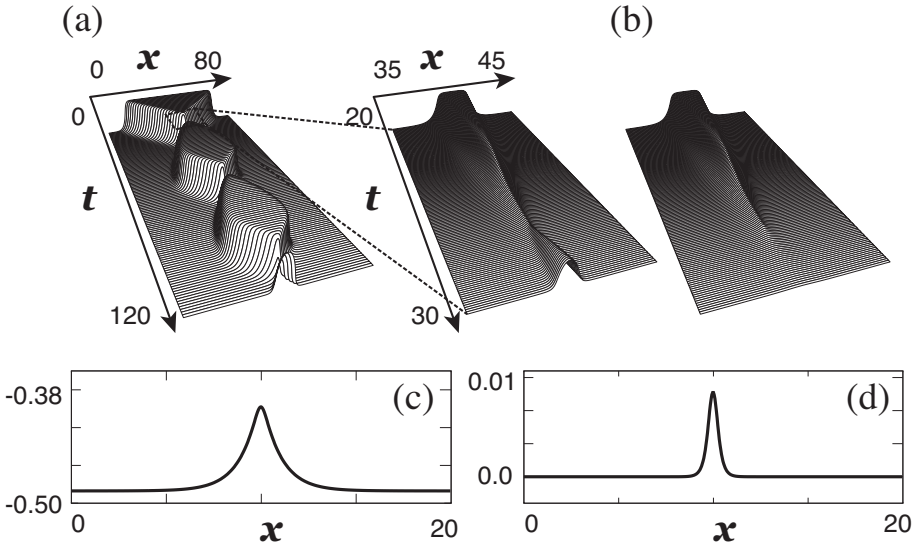

FIGURE 1. (a), (b): Bird-view plot for the colliding interfaces of a front-back pulse observed numerically in the original RD system (1) with $\vartheta(x) = \varsigma$. The horizontal and vertical axes represent the space and the time, respectively and only $v(x,t)$ is shown. Transition from standing breather to annihilation occurs when $\varsigma = \varsigma_s \approx 0.0137267$. The other parameters are set to $(\epsilon, D, \tau) = (0.05, 1.0, 0.160)$. (a) The interfaces collide and the pulse eventually settles down to a standing breather. When ς is slightly larger than ς_s, it settles down to the background constant solution as shown in (b). Just after the collision between the two interfaces, the pulse remains as a small stationary pulse for a certain time. (c) Profile of a codimension one stationary pulse solution and (d) profile of its associated eigenfunction whose unstable eigenvalue is 22.72. In (c) and (d), the profiles of the v component are depicted.

the location of the interface $\phi(t)$ obeys $\dot{\phi}(t) = \theta(v_I)$ ($\theta(v_I) := -v_I/\sqrt{2}\tau$). When Eq.(4) is coupled with the second equation in Eqs.(1) for the v-field, the above v_I is no longer constant but replaced by $v_I = v(\phi(t), t)$, the value of $v(x,t)$ at the interface. This replacement is valid as long as $\epsilon \ll 1$ where the contribution from the spatial variation in v is negligible near the interface. For the pulse solution with two interfaces, we may assume as a 0th-approximation that the solution for u is composed of the superposition of two facing fronts $u = -S(x - \phi_1(t)) + S(x - \phi_2(t)) - P_+$. Accordingly, the values of v for the equation of $\phi_2(t)$ and $\phi_1(t)$ are respectively replaced by $v(\phi_2(t), t)$ and $v(\phi_1(t), t)$, which, after taking the sharp interface limit $\epsilon \to 0$, yields the hybrid system (2). Numerically, it was found that HS (2) approximated the dynamics of the original RD system (1) qualitatively well and the ANN-SB transition was also observed. Straightforward calculation, however, reveals that HS does not have a pulse solution corresponding to the scattor for the RD system.

Lemma 2.1. *There appears only one stationary pulse solution to HS (2) with* $\vartheta(x) \equiv \vartheta$ *where* $0 < \vartheta < 1/2$.

Proof. To seek for the stationary pulse solution, one may follow the same procedure as in the proof of Proposition 2 stated later. The details of the calculation are delegated to the proof and the brief outline is sketched here: For the stationary pulse solution, the time derivatives in the three equations in (2) are set to 0 (i.e., $\dot{\phi}_2 = \dot{\phi}_1 = v_t = 0$). The third equation v is solved first, and then the v is used for $v(\phi_2)$ and $v(\phi_1)$ in the first and the second equations, which yields the value of the pulse width h_0 uniquely given by $h_0 = -\sqrt{D}\log 2\vartheta$. □

Actually for the RD system, it is numerically confirmed that there appear two stationary pulse solutions, the smaller of which is the scattor for the ANN-SB transition. The solution stated in the above lemma corresponds to the larger one and the smaller one is absent, which gave rise to some discrepancy about the ANN regimes of the two systems. See [12] for details.

The objective in this section is to modify the hybrid system so that there appears a counterpart to the above-mentioned scattor for the RD system. It should be noted that, in the derivation of HS, no interaction was taken into account between the two interfaces of the u-component. For the purpose of the modification, therefore, we will take this interaction into account and rederive the equations for ϕ_2 and ϕ_1. Here again, we assume that the solution for u is approximated by the superposition of two fronts as

$$u = -S(x - \phi_1(t)) + S(x - \phi_2(t)) - P_+ + V(x,t)\ . \tag{5}$$

This time, the fronts are well separated and interact weakly. The term $V(x,t)$ ($||V||_2 \ll 1$) represents the deviation of the superposed fronts from the exact solution. Furthermore, we assume that the two interfaces move as $\dot{\phi}_1(t) = -\theta_1 + \dot{l}_1(t)$ and $\dot{\phi}_2(t) = \theta_2 + \dot{l}_2(t)$ ($|\dot{l}_1|, |\dot{l}_2| \ll 1$) with $\theta_1 := \theta(v_1)$, $\theta_2 := \theta(v_2)$ (Fig. 2). Our goal is to obtain the time-evolution equations for $l_1(t)$ and $l_2(t)$, which come from the weak front interaction. For the moment, we suppose that the equation for u in Eqs. (1) is uncoupled with that for v, and we treat v_1 and v_2 as constant, which, when coupled with the v-field, vary as $v_1 = v(\phi_1(t), t)$ and $v_2 = v(\phi_2(t), t)$. In what follows, we focus on the left interface and derive an equation for $l_1(t)$. Note that the approximations to be made in the calculation below are valid only near the left interface $x = \phi_1$. In the moving coordinate $z = x - \phi_1(t)$, the equation (4) with $v = v_1$ and the ansatz (5) are respectively rewritten as

$$\tau\epsilon(-\dot{\phi}_1\ u_z + u_t) = \epsilon^2 u_{xx} + f(u; v_1), \tag{6}$$

$$u = -S(z) + S(z-h) - P_+ + \tilde{V}(z,t)\ , \tag{7}$$

where $h := \phi_2 - \phi_1$ represents the pulse width and $\tilde{V}(z,t) := V(x + \phi_1, t)$. Substituting Eq. (7) into Eq. (6), we have

$$\begin{aligned} &\tau\epsilon(-\theta_1 + \dot{l}_1)S_z(z) + \tau\epsilon(-\theta_2 - \dot{l}_2)S_z(z-h) + \tau\epsilon(\theta_1 - \dot{l}_1)\tilde{V}_z(z,t) + \tau\epsilon\tilde{V}_t(z,t) \\ &= \epsilon^2\{-S_{zz}(z) + S_{zz}(z-h) + \tilde{V}_{zz}(z,t)\} + f(-S(z) + S(z-h) - P_+; v_1) \\ &\quad + f_u(-S(z) + S(z-h) - P_+; v_1)\tilde{V}(z,t) + h.o.t.\ , \end{aligned} \tag{8}$$

where $h.o.t.$ denotes higher order terms. The equation is transformed further as

$$\begin{aligned}\tau\epsilon\tilde{V}_t(z,t) =&\epsilon^2\tilde{V}_{zz}(z,t) - \tau\epsilon\theta_1\tilde{V}_z(z,t) + f_u(-S(z)+S(z-h)-P_+;v_1)\tilde{V}(z,t)\\ &- \{\epsilon^2 S_{zz}(z) - \tau\epsilon\theta_1 S_z(z)\} + \{\epsilon^2 S_{zz}(z-h) + \tau\epsilon\theta_2 S_z(z-h)\}\\ &+ f(-S(z)+S(z-h)-P_+;v_1) + f(S(z-h);v_2) - f(S(z-h);v_2)\\ &- \tau\epsilon\dot{l_1}S_z(z) + \tau\epsilon\dot{l_2}S_z(z-h) + h.o.t.\\ =&\ \epsilon^2\tilde{V}_{zz}(z,t) - \tau\epsilon\theta_1\tilde{V}_z(z,t) + f_u(-S(z);v_1)\tilde{V}(z,t)\\ &- \{\epsilon^2 S_{zz}(z) - \tau\epsilon\theta_1 S_z(z) + f(S(z);-v_1)\}\\ &+ \{\epsilon^2 S_{zz}(z-h) + \tau\epsilon\theta_2 S_z(z-h) + f(S(z-h);v_2)\}\\ &+ f_u(-S(z);v_1)\times\{S(z-h)-P_+\} - f_u(P_+;v_2)\times\{S(z-h)-P_+\}\\ &- \tau\epsilon\dot{l_1}S_z(z) + \tau\epsilon\dot{l_2}S_z(z-h) + h.o.t.\\ =&\ \{\epsilon^2\frac{\partial^2}{\partial z^2} - \tau\epsilon\theta_1\frac{\partial}{\partial z} + f_u(-S(z);v_1)\}\tilde{V}(z,t)\\ &+ \{f_u(-S(z);v_1) - f_u(P_+;v_2)\}\times\{S(z-h)-P_+\}\\ &- \tau\epsilon\dot{l_1}S_z(z) + \tau\epsilon\dot{l_2}S_z(z-h) + h.o.t.\ ,\end{aligned} \tag{9}$$

where we used

$$\begin{cases} f(-S(z)+S(z-h)-P_+;v_1) \approx f(-S(z);v_1) + f_u(-S(z);v_1)\ \{S(z-h)-P_+\},\\ f(S(z-h);v_2) = f(P_+ + S(z-h) - P_+;v_2)\\ \qquad\qquad \approx f(P_+;v_2) + f_u(P_+;v_2)\ \{S(z-h)-P_+\}, \end{cases} \tag{10}$$

$$\begin{cases} \epsilon^2 S_{zz} - \tau\epsilon\theta_1 S_z + f(S;-v_1) = 0,\\ \epsilon^2 S_{zz} + \tau\epsilon\theta_2 S_z + f(S;v_2) = 0. \end{cases} \tag{11}$$

Since v_1 and v_2 are respectively given by $v_1 = v(\phi_1(t),t)$ and $v_2 = v(\phi_2(t),t)$ when Eq.(4) is coupled with the v-field, it follows that $v \to -v$ results in $v_1 \to -v_1$ and $v_2 \to -v_2$, which transforms Eq.(9) further as

$$\begin{aligned}\tau\epsilon\tilde{V}_t(z,t) = &\{\epsilon^2\frac{\partial^2}{\partial z^2} + \tau\epsilon\theta_1\frac{\partial}{\partial z} + f_u(S(z);v_1)\}\tilde{V}(z,t)\\ &+ \{f_u(S(z);v_1) - f_u(-P_+;v_2)\}\times\{S(z-h)-P_+\}\\ &- \tau\epsilon\dot{l_1}S_z(z) + \tau\epsilon\dot{l_2}S_z(z-h) + h.o.t.\ ,\end{aligned} \tag{12}$$

where we used the property $f_u(-u,-v) = f_u(u,v)$. Let us rewrite the above equation for $\tilde{V}$ as

$$\tau\epsilon\tilde{V}_t(z,t) = L\tilde{V}(z,t) + g(z,t), \tag{13}$$

where

$$\begin{aligned} L :=&\epsilon^2\frac{\partial^2}{\partial z^2} + \tau\epsilon\theta_1\frac{\partial}{\partial z} + f_u(S(z);v_1),\\ g :=&\{f_u(S(z);v_1) - f_u(-P_+;v_2)\}\ \{S(z-h)-P_+\}\\ &- \tau\epsilon\dot{l_1}S_z(z) + \tau\epsilon\dot{l_2}S_z(z-h) + h.o.t.\ .\end{aligned} \tag{14}$$

The deviation $\tilde{V}$ is bounded in time t if and only if

$$\langle\phi^*(z;v_1), g(z,t)\rangle = 0 \tag{15}$$

where $\phi^*(z;v_1)$ is the zero eigenfunction of the adjoint operator

$$L^* := \epsilon^2 \frac{\partial^2}{\partial z^2} - \tau\epsilon\theta_1 \frac{\partial}{\partial z} + f_u(S(z);v_1). \tag{16}$$

That is, $\phi^*(z;v_1)$ holds for $L^*\phi^*(z;v_1)=0$ and it is explicitly given by $\phi^*(z;v_1) = \exp\left(-v_1 z/\sqrt{2}\epsilon\right)\ S_z(z)$. The orthogonality condition (15) is called the solvability condition in which the deviation $\tilde{V}$ should not contain any component in the direction of the translation mode S_z to eliminate the secular term increasing with t [10].

In this paper, we derive equations of motion of the two interfaces by formal argument, assuming the existence of an attractive invariant manifold on which the reduced dynamics is described. The rigorous justification is shown in [4]. Thus, Eq.(15) becomes,

$$\tau \dot{l_1} M_0(v_1) = M_1(v_1, v_2), \tag{17}$$

where $M_0(v) := \langle \phi^*(z;v_1), S_z(z)\rangle$. Note that the range of v we are concerned with is $-1 < v_1 < 1$ so that $\phi^*(z;v_1)$ decays for $z \to \pm\infty$. We have neglected the term $\langle \phi^*(z;v_1), S_z(z-h)\rangle$ since both $\phi^*(z;v_1)$ and $S_z(z)$ are localized around $z=0$ and decay exponentially fast as $\exp(-|z|/\epsilon)$. The function $M_1(v_1,v_2)$ is given by

$$\begin{aligned} M_1(v_1,v_2) = &-2\int_{-\infty}^{+\infty} \left[\frac{3}{(e^x+e^{-x})^2} + v_1 \frac{e^{-x}}{e^x+e^{-x}}\right] \\ &\times \{S(2\sqrt{2}\epsilon x - h) - P_+\}\ \frac{e^{-2v_1 x}}{(e^x+e^{-x})^2}\ dx \\ &-(v_2-v_1)\int_{-\infty}^{+\infty} \{S(2\sqrt{2}\epsilon x - h) - P_+\}\ \frac{e^{-2v_1 x}}{(e^x+e^{-x})^2} dx, \end{aligned} \tag{18}$$

which contributes only when $h \sim \mathcal{O}(\epsilon)$. Recalling that v_1 and v_2 represent the values of $v(x,t)$ at the interfaces when coupled with the v-field, we may neglect the second term in $M_1(v_1,v_2)$ since $v_2 - v_1 \sim \mathcal{O}(\epsilon)$ when $h \sim \mathcal{O}(\epsilon)$. Then, $M_1(v_1,v_2)$ in Eq. (18) reduces to

$$\begin{aligned} M_1(v_1,v_2) \ &\approx\ -2\int_{-\infty}^{+\infty} \left[\frac{3}{(e^x+e^{-x})^2} + v_1 \frac{e^{-x}}{e^x+e^{-x}}\right] \\ &\quad\times \{S(2\sqrt{2}\epsilon x - h) - P_+\} \frac{e^{-2v_1 x}}{(e^x+e^{-x})^2} dx \\ &\approx 2\left(\int_{-\infty}^{+\infty} \left[\frac{3}{(e^x+e^{-x})^2} + v_1 \frac{e^{-x}}{e^x+e^{-x}}\right] \frac{e^{(2-2v_1)x}}{(e^x+e^{-x})^2} dx\right)\ e^{-\frac{h}{\sqrt{2}\epsilon}} \\ &=: M_1(v_1)\ e^{-\frac{h}{\sqrt{2}\epsilon}}, \end{aligned} \tag{19}$$

where we used $S(2\sqrt{2}\epsilon x - h) - P_+ \approx -e^{2x}\ e^{-\frac{h}{\sqrt{2}\epsilon}}$ for $x \to -\infty$. Thus, from Eq. (17), we obtain the equation for ϕ_1

$$\dot{\phi_1} = \frac{v_1}{\sqrt{2}\tau} + \frac{M(v_1)}{\tau}\ e^{-\frac{h}{\sqrt{2}\epsilon}}. \tag{20}$$

Quite similarly, the equation for ϕ_2 is obtained as

$$\dot{\phi_2} = -\frac{v_2}{\sqrt{2}\tau} - \frac{M(v_2)}{\tau}\ e^{-\frac{h}{\sqrt{2}\epsilon}}. \tag{21}$$

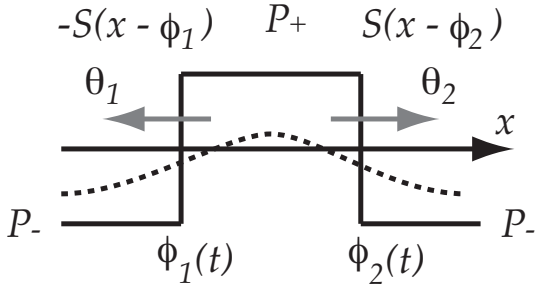

FIGURE 2. Schematic figure for a pulse constructed by two front solutions. We set $\phi_1(t) = -\theta_1 t + l_1(t)$ and $\phi_2(t) = \theta_2 t + l_2(t)$ where $\theta_1 := \theta(v_1)$ and $\theta_2 := \theta(v_2)$ are treated as constant, which vary with time when the scalar equation (4) is coupled with the v-field (indicated by the dotted line).

The function $M(v)$ is explicitly given by

$$\begin{cases} M(v) = M_1(v)/M_0(v), \\ M_0(v) = \sqrt{2}\displaystyle\int_{-\infty}^{+\infty} \frac{e^{-2vx}}{(e^x + e^{-x})^4} dx, \\ M_1(v) = 2\displaystyle\int_{-\infty}^{+\infty} \left[\frac{3}{(e^x + e^{-x})^2} + v\frac{e^{-x}}{e^x + e^{-x}} \right] \frac{e^{(2-2v)x}}{(e^x + e^{-x})^2}\, dx. \end{cases} \tag{22}$$

When Eq.(4) is coupled with the v-field, the above v_1 and v_2 are replaced by $v_1 = v(\phi_1(t), t)$ and $v_2 = v(\phi_2(t), t)$, respectively. The equation for v remains unchanged from HS (2).

3. **Analysis of modified hybrid system.** By the computation demonstrated in the previous section, we arrive at the following proposition:

Proposition 1. *The motion of the interfaces $x = \phi_2(t)$, $\phi_1(t)$ $(\phi_2(t) \geq \phi_1(t))$ of the pulse solution to Eqs. (1) with $\vartheta(x) \equiv \vartheta$ is approximately described by*

$$\begin{cases} \dot{\phi}_2 = -\dfrac{v(\phi_2, t)}{\sqrt{2}\tau} - \dfrac{M(v(\phi_2, t))}{\tau} e^{-\frac{h}{\sqrt{2}\epsilon}}, \\ \dot{\phi}_1 = \dfrac{v(\phi_1, t)}{\sqrt{2}\tau} + \dfrac{M(v(\phi_1, t))}{\tau} e^{-\frac{h}{\sqrt{2}\epsilon}}, \\ v_t = Dv_{xx} + u(x; \phi_2, \phi_1) - v + \vartheta, \end{cases} \tag{23}$$

where $h(t) := \phi_2(t) - \phi_1(t)$, and the definitions of $u(x; \phi_2, \phi_1)$ and $M(v)$ are given in Eqs. (3) and (22), respectively.

Let us call this system a modified hybrid system (mHS) hereafter. Notice the interaction term $M(v)\, e^{-h/\sqrt{2}\epsilon}/\tau$ in the equations for ϕ_2 and ϕ_1 in mHS (23), which was absent in HS (2). In this section, we investigate the existence and stability of stationary pulse solution for mHS. As for the existence, the following proposition holds:

Proposition 2. *Let the stationary pulse solution to Eqs. (23) be denoted by* $(\phi_2(t), \phi_1(t), v(x,t)) = (\phi_2^{(0)}, \phi_1^{(0)}, v^{(0)}(x))$. *The pulse width* $h_0 := \phi_2^{(0)} - \phi_1^{(0)}$ *and the value of* $v^{(0)}(x)$ *at the interfaces* $V := v^{(0)}(\phi_1^{(0)}) = v^{(0)}(\phi_2^{(0)})$ *satisfy the relations* $h_0 = -\sqrt{2}\epsilon \log\left(-V/\sqrt{2}M\,(V)\right)$ *and* $V = \vartheta - e^{-h_0/\sqrt{D}}/2$.

Proof. The equation for $v^{(0)}(x)$ is readily solved as

$$v^{(0)}(x) = \begin{cases} \left(-\frac{1}{2}e^{(x-\phi_2^{(0)})/\sqrt{D}} + \frac{1}{2}e^{(x-\phi_1^{(0)})/\sqrt{D}}\right) + \left(-\frac{1}{2} + \vartheta\right) & \left(x \le \phi_1^{(0)}\right), \\ \left(-\frac{1}{2}e^{(x-\phi_2^{(0)})/\sqrt{D}} - \frac{1}{2}e^{-(x-\phi_1^{(0)})/\sqrt{D}}\right) + \left(\frac{1}{2} + \vartheta\right) & \left(\phi_1^{(0)} \le x \le \phi_2^{(0)}\right), \\ \left(\frac{1}{2}e^{-(x-\phi_2^{(0)})/\sqrt{D}} - \frac{1}{2}e^{-(x-\phi_1^{(0)})/\sqrt{D}}\right) + \left(-\frac{1}{2} + \vartheta\right) & \left(\phi_2^{(0)} \le x\right), \end{cases} \tag{24}$$

from which we have $v^{(0)}(\phi_2^{(0)}) = v^{(0)}(\phi_1^{(0)}) = -e^{-h_0/\sqrt{D}}/2 + \vartheta =: V$, where $h_0 := \phi_2^{(0)} - \phi_1^{(0)}$. On the other hand, the first and the second equations in Eqs. (23) are transformed as $h_0 = -\sqrt{2}\epsilon \log\left(-v^{(0)}(\phi_i^{(0)})\,/\sqrt{2}M\left(v^{(0)}(\phi_i^{(0)})\right)\right) \quad (i = 1, 2)$, giving $h_0 = -\sqrt{2}\epsilon \log\left(-V/\sqrt{2}M(V)\right)$, which completes the proof. □

Figure 3(a) shows the two graphs in the (V, h_0) plane. Note that each intersection corresponds to the existence of a stationary pulse solution. We see that the graphs are tangent to each other at some ϑ, indicating that a pair of pulse solutions are created simultaneously. By changing ϑ, we obtain the existence curve for the stationary pulse solution (Fig. 3(b)). From this curve, it is found that a pair of pulses are created via a saddle-node bifurcation (Fig. 4(a)) and that the pulse width of the larger one diverges at $\vartheta = 0$, while that of the smaller one continues to exist for $\vartheta < 0$. We remark that the larger one corresponds to the only stationary pulse solution to HS stated in Lemma 2.1.

Following [9], we can also investigate the stability of these pulse solutions.

Proposition 3. *The linear stability of the stationary pulse solution to Eqs. (23) is determined by the spectrum* λ *of the following equations*

$$\begin{cases} Ae^{-\kappa h_0} + A + 2\sqrt{2}\tau D\kappa\lambda - 2D\kappa AV' + 4D\kappa B = 0, \\ Ae^{-\kappa h_0} - A - 2\sqrt{2}\tau D\kappa\lambda + 2D\kappa AV' = 0, \end{cases} \tag{25}$$

where h_0 *and* V *are defined in Proposition 2 and* $V' := -v_x^{(0)}(\phi_2^{(0)}) = v_x^{(0)}(\phi_1^{(0)}) = (1/2 + V - \vartheta)/\sqrt{D}$ *. The constants* A, B *and* κ *are given by* $A = 1 - VM_v(V)/M(V)$ $(M_v(v) := dM(v)/dv\ )$, $B = V/\sqrt{2}\epsilon$ *and* $\kappa = \sqrt{(1+\lambda)/D}$ $(\Re(\kappa) > 0\ )$, *respectively.*

Proof. Linearizing Eqs. (23) about the stationary solution by substituting $\phi_2(t) = \phi_2^{(0)} + \psi_2(t)$, $\phi_1(t) = \phi_1^{(0)} - \psi_1(t)$, $v(x,t) = v^{(0)}(x) + w(x,t) \quad (|\psi_2|, |\psi_1|, ||w||_2 \ll 1)$ and putting $\dot{\psi}_2 = \lambda\psi_2$, $\dot{\psi}_1 = \lambda\psi_1$ and $w_t = \lambda w$, we obtain the eigenvalue problem for λ:

$$\begin{cases} -\sqrt{2}\tau\ \lambda\psi_2 = \ \{-V'\psi_2 + w(\phi_2^{(0)})\} + \sqrt{2}\ \{\ -M_v(V)V'\psi_2 \\ \qquad\qquad +M_v(V)w(\phi_2^{(0)}) - M(V)(\psi_2 + \psi_1)/\sqrt{2}\epsilon\ \}e^{-h_0/\sqrt{2}\epsilon}, \\ \sqrt{2}\tau\ \lambda\psi_1 = \ \{\ \ V'\psi_1 - w(\phi_1^{(0)})\} - \sqrt{2}\ \{\ -M_v(V)V'\psi_1 \\ \qquad\qquad +M_v(V)w(\phi_1^{(0)}) - M(V)(\psi_2 + \psi_1)/\sqrt{2}\epsilon\ \}e^{-h_0/\sqrt{2}\epsilon}, \\ \qquad \lambda w = Dw_{xx} - w - \psi_1\ \delta(x - \phi_1^{(0)}) + \psi_2\ \delta(x - \phi_2^{(0)}), \end{cases} \tag{26}$$

where $V' := -v_x^{(0)}(\phi_2^{(0)}) = v_x^{(0)}(\phi_1^{(0)}) = (1/2+V-\vartheta)/\sqrt{D}$ and $M_v(v) := dM(v)/dv$. The solution to the third equation is given by the C^0-function

$$w(x) = \begin{cases} -\dfrac{\psi_1}{2D\kappa}e^{\kappa(x-\phi_1^{(0)})} + \dfrac{\psi_2}{2D\kappa}e^{\kappa(x-\phi_2^{(0)})} & \left(x \le \phi_1^{(0)}\right), \\ -\dfrac{\psi_1}{2D\kappa}e^{-\kappa(x-\phi_1^{(0)})} + \dfrac{\psi_2}{2D\kappa}e^{\kappa(x-\phi_2^{(0)})} & \left(\phi_1^{(0)} \le x \le \phi_2^{(0)}\right), \\ -\dfrac{\psi_1}{2D\kappa}e^{-\kappa(x-\phi_1^{(0)})} + \dfrac{\psi_2}{2D\kappa}e^{-\kappa(x-\phi_2^{(0)})} & \left(\phi_2^{(0)} \le x\right), \end{cases} \tag{27}$$

where $\kappa = \sqrt{(1+\lambda)/D}$ $(\Re(\kappa) > 0)$. Substituting $w(\phi_2^{(0)})$ and $w(\phi_1^{(0)})$ into the first and second equations and demanding that the equations for ψ_2 and ψ_1 have nontrivial solution $(\psi_2, \psi_1) \neq (0,0)$ result in the equations in (25). □

The first and the second equations in Eqs. (25) corresponds to a symmetric and an asymmetric mode, respectively. Note that $\lambda = 0$ always satisfies the second equation, which comes from the translational invariance of the pulse solution. The stability of the pulse solutions is also shown in Fig.3(b). As ϑ is decreased, the larger pulse changes its stability via two Hopf bifurcations, while the smaller one is always unstable with one positive real eigenvalue. This bifurcation structure qualitatively agrees with that obtained numerically for the RD system (1). The reader is referred to Fig.17 in [12]. The smaller pulse solution corresponds to the small pulse solution observed for the RD system, which, as we saw in section 1, plays a crucial role in determining the asymptotic behavior for the ANN-SB transition.

The eigenfunctions are given by Eqs. (27), where, without loss of generality, we may set $\psi_2 = -\psi_1 = 1$ for the symmetric mode and $\psi_2 = \psi_1 = 1$ for the asymmetric mode. Figure 4(b) shows the eigenfunction associated with the unstable mode for the small pulse solution. Numerically, the ANN-SB transition is observed also for mHS. Therefore, it is quite plausible that, just as in the RD case, the small unstable stationary solution plays the role of a scattor in the ANN-SB transition, and that it settles down to either the SB solution or the background state when perturbed along this unstable mode.

4. **Concluding remarks and discussion.** In our previous paper [12], we numerically confirmed that the hybrid system (2) successfully described the motion of a front-back pulse for the PDE system, except for the annihilation dynamics, and in this short article, we modified the hybrid system and investigated the modified system (23) for the existence and stability of the stationary pulse solution. The results we demonstrated formally here seem to suggest that the modified hybrid system has the potential for describing the interface dynamics even during the collision process with large deformation of the pulse profile. Therefore, it would be worth exploring further the validity of the weak interaction framework, which, with some restrictions on the time interval or initial condition, for instance, might enable us to consider the annihilation dynamics rigorously[4][16].

In deriving the modified system, we assumed that the u-component of the pulse solution is composed of two weakly interacting interfaces, and that its profile is always given by the rectangular function $u(x; \phi_2^{(0)}, \phi_1^{(0)})$ in Eq. (3). The existence of invariant manifold has not yet been proven for singular limit system including such discontinuous functions. Supposing it with some smoothness, we obtained

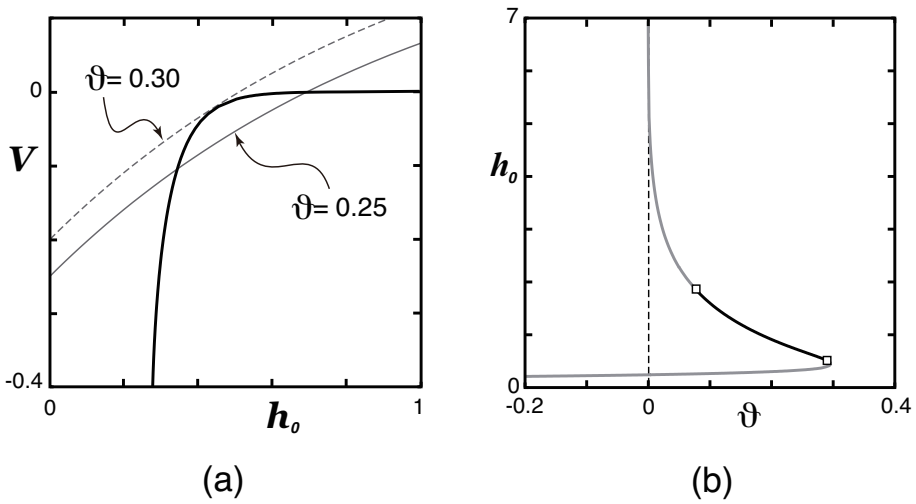

FIGURE 3. (a) The two graphs of $h_0 = -\sqrt{2}\epsilon \log(-V/\sqrt{2}M(V))$ (solid black) and $V = \vartheta - e^{-h_0/\sqrt{D}}/2$ (solid or broken gray). The vertical axis is the value of $v^{(0)}$ at the interface V and the horizontal axis is the pulse width h_0. Each intersection corresponds to a stationary pulse solution. For $\vartheta \approx 0.3$, the graphs are tangent (broken gray curve) and they have two intersections for $\vartheta < 0.3$ (solid gray curve). (b) By changing ϑ and plotting h_0 of the intersections of the two graphs in (a), we obtain a bifurcation curve for the stationary pulse solution for mHS (23). A pair of pulse solutions are created via a saddle-node bifurcation around $\vartheta = 0.3$, the larger of which diverges in width at $\vartheta = 0$. On the other hand, the smaller one continues to exist for $\vartheta < 0$. Furthermore, the spectrum obtained from Eqs. (25) for linear stability reveals that, as ϑ is varied, the larger pulse undergoes Hopf bifurcations twice (indicated by the open squares) and that the smaller one is always unstable with one positive real eigenvalue. The black and gray curves indicate stable and unstable solutions, respectively. The other parameters are fixed as $\tau = 0.160$, $D = 1.0$, $\epsilon = 0.05$.

the equation of motion for a front-back pulse in terms of the two separated interfaces (ϕ_1, ϕ_2). The reduced flow provides an understanding of qualitative dynamical changes in orbital behaviors near an invariant set depending on one or more parameters. Nevertheless, the modified hybrid system (23) reproduced qualitatively the same bifurcation structure for the stationary pulse solution (compare Fig. 3(b) with Fig.17 in [12]).

In particular, we obtained the explicit form of $M(v)$, the coefficient of the interaction term whose sign determines whether the interaction is attractive or repulsive. Figure 4(c) shows the graph of $M(v)$ given by Eq. (22) with respect to the value of v, in which all the curves are positive.

Remark 1. $M_0(v)$ diverge at $v = \pm 2$ and $M_1(v)$ at $v = -1$ and 2. $M(v)$ also diverges at $v = -1$ and decreases monotonically to $M(2) = 2\sqrt{2}$. Especially, the

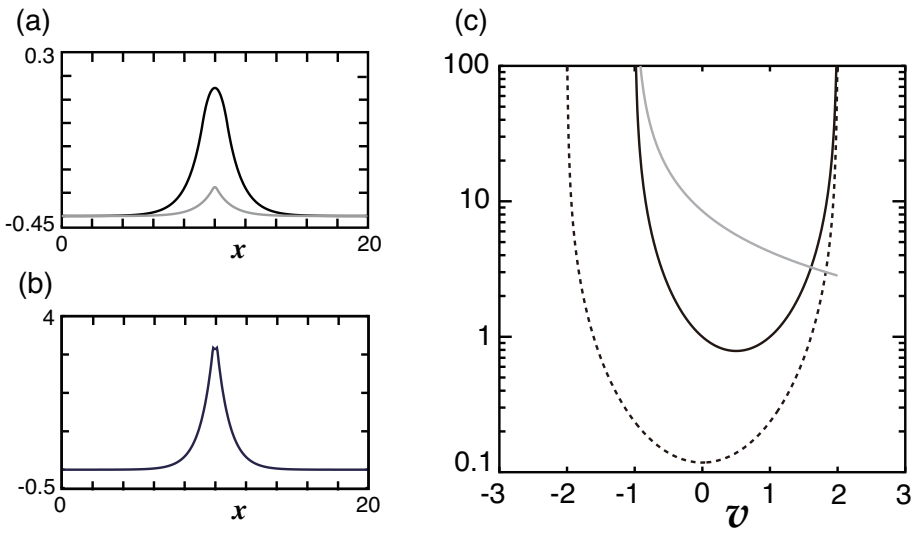

FIGURE 4. (a) The profiles of large (black) and small (gray) stationary pulse solutions obtained from Eqs. (24) for $\vartheta = 0.1$. The other parameters are the same as in Fig. 3. For the u-component, the profiles of these pulse solutions are both given by the rectangular function $u(x; \phi_2^{(0)}, \phi_1^{(0)})$ in Eq. (3). From the bifurcation curve in Fig. 3(b), we see that the large pulse is stable, while the small one is unstable. (b) The profile of eigenfunction associated with the unstable real eigenvalue of the small pulse solution. (c) The graphs of $M_0(v)$ (broken curve), $M_1(v)$ (gray solid curve) and $M(v)$ (black solid curve) in Eq. (22).

coefficient $M(v)$ is positive for the range of v we are concerned with, which indicates that the interaction terms serve to attract the interfaces at all times and facilitate the interface annihilation, reproducing the phase diagram of pulse behaviors quantitatively closer to those observed in the original RD system.

Note that, unlike in the RD case, the profile of the u-component does not vanish even after the collision for both of the hybrid systems (2) and (23), so that we supposed that annihilation occurred when the pulse interfaces crossed (i.e., $\phi_2 = \phi_1$) in numerical simulations. With this definition of annihilation, the ANN-SB transition was observed also for (2), the hybrid system without interaction terms, in some parameter regime where the interfaces collided with relatively high velocity. This implies that annihilation mechanism for (2) is totally different from that observed in the modified hybrid system (23) as well as the original RD system, where the unstable pulse solution is a key to understanding the underlying mechanism behind the ANN-SB transition. What was demonstrated in this paper is that the modification reproduced the same bifurcation structure for the stationary pulse solution qualitatively, hence a counterpart to the separator observed in numerics for the original RD system.

For the modified hybrid system to be used to study the strong collision process, we should give analytical answers to the above questions and implications and clarify

to what extent and under what conditions it approximates the original RD system well.

Acknowledgments. This work was supported in part by a Grant-in-Aid for Scientific Research (B) (No. 24340019) to S.-I. E. and (A) (No. 26747015) to Y. N.

REFERENCES

[1] M. Argentina, P. Coullet and V. Krinsky, Head-on collisions of waves in an excitable FitzHugh-Nagumo system: a transition from wave annihilation to classical wave behavior, *J. theor. Biol.,* **205** (2000), 47–52.
[2] M. Argentina, P. Coullet and L. Mahadevan, Colliding waves in a model excitable medium: Preservation, annihilation, and bifurcation, *Phys. Rev. Lett.,* **79** (1997), 2803–2806.
[3] X. Chen, S.-I. Ei and M. Mimura, Self-motion of camphor discs. Model and analysis, *Networks and Heterogeneous Media,* **4** (2009), 1–18.
[4] S.-I. Ei, The motion of weakly interacting pulses in reaction-diffusion systems, *J. Dyn. Diff. Eq.,* **14** (2002), 85–137.
[5] S.-I. Ei, H. Ikeda and T. Kawana, Dynamics of front solutions in a specific reaction-diffusion system in one dimension, *Jpn. J. Indust. Appl. Math.,* **25** (2008), 117–147.
[6] S.-I. Ei, M. Mimura and M. Nagayama, Pulse-pulse interaction in reaction-diffusion systems, *Physica D,* **165** (2002), 176–198.
[7] P. C. Fife, *Dynamics of Internal Layers and Diffusive Interface,* 1st edition, Society for Ind. and Appl. Math., Pennsylvania, 1988.
[8] Y. Fukao, Y. Morita and H. Ninomiya, Some entire solutions of the Allen-Cahn equation, *Taiwanese J. Math.,* **8** (2004), 15–32.
[9] H. Ikeda, T. Ikeda and M. Mimura, Hopf bifurcation of travelling pulses in some bistable reaction-diffusion systems, *Methods and Appl. of Anal.,* **7** (2000), 165–193.
[10] Y. Kuramoto, Instability and turbulence of wavefronts in reaction-diffusion systems, *Prog. Theor. Phys.,* **63** (1980), 1885–1903.
[11] Y. Morita and Y. Mimoto, Collision and collapse of layers in a 1D scalar reaction-diffusion equation, *Physica D,* **140** (2000), 151–170.
[12] K. Nishi, Y. Nishiura and T. Teramoto, Dynamics of two interfaces in a hybrid system with jump-type heterogeneity, *Jpn. J. Ind. App. Math.,* **30** (2013), 351–395.
[13] Y. Nishiura, T. Teramoto and K.-I. Ueda, Scattering and separators in dissipative systems, *Phys. Rev. E,* **67** (2003), 056210-1–056210-7.
[14] Y. Nishiura, T. Teramoto and K.-I. Ueda, Scattering of traveling spots in dissipative systems, *Chaos,* **15** (2005), 047509, 10pp.
[15] T. Ohta, M. Mimura and R. Kobayashi, Higher-dimensional localized patterns in excitable media, *Physica D,* **34** (1989), 115–144.
[16] A. Scheel and J. Wright, Colliding dissipative pulses – the shooting manifold, *J. Diff. Eqs.,* **245** (2008), 59–79.
[17] H. Yagisita, Backward global solutions characterizing annihilation dynamics of travelling fronts, *Publ. RIMS, Kyoto Univ.,* **39** (2003), 117–164.

Received January 2014; revised June 2014.

E-mail address: Eichiro@math.sci.hokudai.ac.jp
E-mail address: k-nishi@es.hokudai.ac.jp
E-mail address: nishiura@wpi-aimr.tohoku.ac.jp
E-mail address: teramoto@asahikawa-med.ac.jp